

Transduction of the scorpion toxin maurocalcine into cells. Evidence that the toxin crosses the plasma membrane.

Eric Estève, Kamel Mabrouk, Alain Dupuis, Sophia Smida-Rezgui, Xavier Altafaj, Didier Grunwald, Jean-Claude Platel, Nicolas Andreotti, Isabelle Marty, Jean-Marc Sabatier, et al.

▶ **To cite this version:**

Eric Estève, Kamel Mabrouk, Alain Dupuis, Sophia Smida-Rezgui, Xavier Altafaj, et al.. Transduction of the scorpion toxin maurocalcine into cells. Evidence that the toxin crosses the plasma membrane.. Journal of Biological Chemistry, 2005, 280 (13), pp.12833-9. 10.1074/jbc.M412521200 . inserm-00381740

HAL Id: inserm-00381740

https://inserm.hal.science/inserm-00381740

Submitted on 10 Jun 2009

HAL is a multi-disciplinary open access archive for the deposit and dissemination of scientific research documents, whether they are published or not. The documents may come from teaching and research institutions in France or abroad, or from public or private research centers.

L'archive ouverte pluridisciplinaire **HAL**, est destinée au dépôt et à la diffusion de documents scientifiques de niveau recherche, publiés ou non, émanant des établissements d'enseignement et de recherche français ou étrangers, des laboratoires publics ou privés.

Transduction of the scorpion toxin maurocalcine into cells. Evidence that the toxin crosses the plasma membrane

Estève Eric [1 2], Mabrouk Kamel [2], Dupuis Alain [1], Smida-Rezgui Sophia [1], Altafaj Xavier [1], Grunwald Didier [1], Platel Jean-Claude [1], Andreotti Nicolas [2], Marty Isabelle [1], Sabatier Jean-Marc [2], Ronjat Michel [1], De Waard Michel [1 *]

[1] Canaux calciques , fonctions et pathologies INSERM : U607, CEA : DSV/IRTSV, Université Joseph Fourier - Grenoble I, 17, rue des martyrs 38054 Grenoble,FR

[2] Biochimie - Ingénierie des protéines CNRS : UMR6560, Université de la Méditerranée - Aix-Marseille II, Boulevard Pierre Dramart 13916 Marseille Cedex 20,FR

* Correspondence should be adressed to: Michel De Waard <michel.dewaard@ujf-grenoble.fr>

Abstract

Maurocalcine (MCa) is a 33 amino acid residue peptide toxin isolated from the scorpion Scorpio maurus palmatus. External application of MCa to cultured myotubes is known to produce Ca^{2+} release from intracellular stores. MCa binds directly to the skeletal muscle isoform of the ryanodine receptor, an intracellular channel target of the endoplasmic reticulum, and induces long-lasting channel openings in a mode of smaller conductance. Here, we investigated the way MCa proceeds to cross biological membranes in order to reach its target. A biotinylated derivative of MCa was produced (MCa_b) and complexed with a fluorescent indicator (streptavidine-cyanine 3) in order to follow the cell penetration of the toxin. The toxin complex efficiently penetrated in various cell types without requiring metabolic energy (low temperature) or implicating an endocytosis mechanism. MCa appeared to share the same features as the so-called Cell-Penetrating Peptides (CPP). Our results provide evidence that MCa has the ability to act as a molecular carrier and to cross cell membranes in a rapid manner (1–2 min) making this toxin the first demonstrated example of a scorpion toxin that translocates into cells.

MESH Keywords Amino Acid Sequence ; Biological Transport ; Biotinylation ; Calcium ; chemistry ; Carrier Proteins ; chemistry ; Cell Differentiation ; Cell Line ; Cell Membrane ; drug effects ; metabolism ; Endocytosis ; Endoplasmic Reticulum ; metabolism ; Gene Products, tat ; metabolism ; Humans ; Kinetics ; Microscopy, Confocal ; Models, Molecular ; Molecular Sequence Data ; Muscle, Skeletal ; cytology ; metabolism ; Peptides ; chemistry ; Protein Conformation ; Protein Isoforms ; Protein Transport ; Ryanodine ; metabolism ; Ryanodine Receptor Calcium Release Channel ; chemistry ; Sarcoplasmic Reticulum ; metabolism ; Scorpion Venoms ; metabolism ; pharmacokinetics ; Signal Transduction ; Temperature ; Time Factors

Maurocalcine (MCa) is a 33-mer toxin isolated from the venom of the scorpion Scorpio maurus palmatus. Since its initial isolation (1), MCa was successfully produced by chemical synthesis which allowed the characterization of its biological activity and the solution of its 3-D structure (2). MCa was shown to be one of the most potent effectors of the skeletal muscle ryanodine receptor type 1 (RyR1), an intracellular calcium channel target. The toxin stimulates the binding of [^{3}H]-ryanodine onto RyR1 present in sarcoplasmic reticulum (SR) vesicles (3,4). It induces strong modifications in the gating of RyR1 channels reconstituted in lipid bilayers that are characterized by the appearance of long-lasting sub-conductance states (4,5). MCa application to purified SR vesicles produces Ca^{2+} release which is consistent with these biophysical effects (3,4). Using a calcium imaging approach, it was also shown that the addition of MCa to the extracellular medium of cultured myotubes induces Ca^{2+} release from the SR into the cytoplasm (4). Taken together, these data are coherent with a direct effect of MCa on RyR1. These observations were confirmed with the identification of MCa's binding site on RyR1 which indicates a cytoplasmic localization (6).

According to the [^{1}H]-NMR analysis of MCa, the peptide presents three disulfide bridges (Cys_3-Cys_{17}, Cys_{10}-Cys_{21}, and Cys_{16}-Cys_{32}) and folds along an Inhibitor Cystine Knot (ICK) motif (2). MCa contains three β-strands: from amino acid residues 9-11 (strand 1), 20-23 (strand 2) and 30-33 (strand 3), respectively. The β-strands 2 and 3 form an antiparallel β-sheet. It is a highly basic peptide that contains eleven basic amino acid residues (33% of the molecule composition). Interestingly enough, eight of the eleven basic residues are oriented towards the same face of the molecule (Fig. 1A).

Two pieces of evidence suggest that MCa should be able to cross the plasma membrane to reach its intracellular target. First, MCa has biological activity consistent with the direct activation of RyR1 when added to the extracellular medium. Second, a structural analysis of MCa reveals a stretch of positively charged amino acid residues that is reminiscent of the protein transduction domains (PTD) found in proteins like Tat from the HIV-1 virus (7,8), the Drosophila homeotic transcription factor ANTP (encoded by the antennapedia gene) (9), and the herpes simplex virus type 1 (HSV-1) VP22 transcription vector (10). Synthetic peptides corresponding to these domains are called cell-penetrating peptides (CPP) and have in common to contain many basic residues (arginine and lysine), often oriented towards the same face of the molecule (Fig. 1B). Because of this structural feature, CPP possess the interesting ability to cross biological membranes in a receptor- or transporter-independent manner (11–13). These peptides seem to target the lipid bilayer directly using complementary charges and penetrate the cell through a mechanism called translocation which remains unclear. Three possible models have been put forth in the literature to explain peptide penetration: 1) the inverted-mycelle model (14) with its membrane-destabilization model variant (11), 2) the

carpet model (15), and the pore-formation model (16). Regardless of the precise mode of entry, CPP possess unique features worth mentioning: i) delivery in 100% of the cells (17), ii) delivery in all cell types both in vitro and in vivo (18,19), iii) ability to cross the blood-brain barrier (18), and iv) the possibility to act as carriers and to translocate large compounds, such as proteins and oligonucleotides (20).

The current study was meant to investigate the ability of MCa to penetrate into cells. We show that a biotinylated version of MCa effectively and rapidly enters various cell types and can behave as a good carrier to allow the penetration of larger compounds. As for other CPP, the mechanism of cell penetration is not linked to an endocytotic pathway. We conclude that MCa represents a new class of disulfide-linked CPP and is the first scorpion toxin shown to enter cells.

Materials and Methods

Chemical Synthesis of MCa and biotinylated MCa

N-α-Fmoc-L-amino acids, 4-hydroxymethylphenyloxy resin, and reagents used for peptide synthesis were obtained from Perkin Elmer Life Sciences. N-α-Fmoc-L-Lys(Biotin)-OH was purchased from Neosytem Groupe SNPE. The MCa and biotinylated MCa (MCa_b) were obtained by the solid-phase peptide synthesis (21) using an automated peptide synthesizer (Model 433A, Applied Biosystems Inc.). Peptide chains were assembled stepwise on 0.25 meq of hydroxymethylphenyloxy resin (1% cross-linked; 0.89 meq of amino group/g) using 1 mmol of N-α-Fmoc amino acid derivatives. The side-chain protecting groups were as follows: trityl for Cys and Asn; tert-butyl for Ser, Thr, Glu, and Asp; pentamethylchroman for Arg; and tert-butyloxycarbonyl or Biotin for Lys. N-α-Amino groups were deprotected by treatment with 18 and 20% (v/v) piperidine/N-methylpyrrolidone for 3 and 8 min, respectively. The Fmoc-amino acid derivatives were coupled (20 min) as their hydroxybenzotriazole active esters in N-methylpyrrolidone (4-fold excess). To obtain MCa, aliquot of peptide resin was removed at its corresponding cycle. After peptide chain assembly, the peptide resin (approximately 0.9 g) was treated between 2 and 3 hrs at room temperature in constant shaking with a mixture of trifluoroacetic acid/H_2O/thioanisol/ethanedithiol (88: 5/5/2, v/v) in the presence of crystalline phenol (2.25 g). The peptide mixture was then filtered, and the filtrate was precipitated by adding cold t -butylmethyl ether. The crude peptide was pelleted by centrifugation (3.000 g for 10 min), and the supernatant was discarded. The reduced peptide was then dissolved in 200 mM Tris-HCl buffer, pH 8.3, at a final concentration of 2.5 mM and stirred under air to allow oxidation/folding (between 50 and 72 h, room temperature). The target products, MCa and MCa_b, were purified to homogeneity, first by reversed-phase high pressure liquid chromatography (Perkin Elmer Life Sciences, C18 Aquapore ODS, 20 μm, 250 × 10 mm) by means of a 60-min linear gradient of 0.08% (v/v) trifluoroacetic acid/0–30% acetonitrile in 0.1% (v/v) trifluoroacetic acid/H_2O at a flow rate of 6 ml/min (λ = 230 nm). A second step of purification of MCa and MCa_b was achieved by ion-exchange chromatography on a carboxymethyl cellulose matrix using 10 mM (buffer A) and 500 mM (buffer B) sodium phosphate buffers, pH 9.0 (60-min linear gradient from 0 to 60% buffer B at a flow rate of 1 ml/min). The homogeneity and identity of MCa or MCa_b were assessed by the following: (i) analytical C18 reversed-phase high pressure liquid chromatography (Merck, C18 Li-Chrospher, 5 μm, 4 × 200 mm) using a 60-min linear gradient of 0.08 % (v/v) trifluoroacetic acid/0–60% acetonitrile in 0.1% (v/v) trifluoroacetic acid/H_2O at a flow rate of 1 ml/min; (ii) amino acid analysis after acidolysis (6 N HCl/2% (w/v) phenol, 20 h, 118°C, N_2 atmosphere); and (iii) mass determination by matrix-assisted laser desorption ionization time-of-flight mass spectrometry.

Formation of the MCa_b-streptavidin-cyanine 3 complex

Soluble streptavidin-cyanine 3 (Strept-Cy3, Amersham) was mixed with four molar equivalent of MCa_b (1 mM) for 2 hrs at room temperature in phosphate buffered saline (PBS).

Preparation of heavy SR vesicles

Heavy SR vesicles were prepared following a modified method of Kim and collaborators (22) as described previously (23). Protein concentration was measured by the Biuret method.

Cell cultures

L6 cells

Rat myogenic L6 cells were obtained from the European Collection of Animal Cell Cultures ECACC (clone C5) and cultured in Dulbecco's modified Eagle's medium supplemented with 15% foetal bovine serum (Life technologies, Inc.) and 1% penicillin/streptomycin (Invitrogen). Differentiation of L6 cells was induced by a shift to differentiation medium (DMEM + 5% Horse serum) when they reached confluence, as described previously (24).

CA1 hippocampal neurons

Hippocampuses from neonatal mice (between days 1 and 2 post partum) were dissected, cleaned of meninges and placed in Hanks balanced salt solution (HBSS; Invitrogen). They were transferred into a dissociation medium containing HBSS, 1% penicillin/streptomycin

(Gibco), 2000 units/ml DNase I and 1% (w/v) trypsin/EDTA and incubated at 37°C for 7 min. After sedimentation, the supernatant was removed and the tissue was washed with a HBSS medium containing 1% penicillin/streptomycin. The tissue was gently triturated in HBBS medium containing 2000 units/ml DNase I, 10% foetal bovine serum and 1% penicillin/streptomycin with a plastic pipette until a homogeneous suspension was obtained. After centrifugation at 100 g during 1 min, the cell pellet was resuspended in Neurobasal/B27 medium (Gibco) containing 0.5 mM L-glutamine and 1% penicillin/streptomycin. Cell cultures were seeded at a density of 10^5 cells/cm^2 on culture dishes coated previously with 20 μg/ml poly-L-lysine at 37°C for 2 hrs. After 2 days, 3 μM cytosine arabinoside was added to the cultures to control the proliferation of non-neuronal cells, and 24 hrs later half of the medium was replaced. The culture media were then subsequently changed every other day.

HEK293 cells

Human embryonic kidney cells (HEK293, Gibco) were passaged by 1% trypsin treatment prior to confluence and maintained in DMEM containing 10% (v/v) foetal bovine serum and 1% penicillin/streptomycin (Invitrogen) and were placed into an incubator and 5% CO_2. The culture medium was changed every other day.

[^{3}H]-ryanodine binding assay

Heavy SR vesicles (1 mg/ml) were incubated at 37°C for 2.5 h in an assay buffer composed of 5 nM [^{3}H]-ryanodine, 150 mM NaCl, 2 mM EGTA, 2 mM Ca^{2+} (pCa=5), and 20 mM HEPES, pH 7.4. 100 nM MCa or MCa_b/streptavidine-Cy3 were added prior to the addition of heavy SR vesicles. [^{3}H]-ryanodine bound to heavy SR vesicles was measured by filtration through Whatmann GF/B glass filters followed by three washes with 5 ml of ice-cold washing buffer composed of 150 mM NaCl, 20 mM HEPES, pH 7.4. [^{3}H]-ryanodine retained on the filters was measured by liquid scintillation. Non-specific binding was measured in the presence of 20 μM unlabeled ryanodine. The data are presented as the mean ± S.E.M. Each experiment was performed in triplicate and repeated at least twice.

Ca^{2+} Release Measurements

Ca^{2+} release from heavy SR vesicles was measured using the Ca^{2+}-sensitive dye, antipyrylazo III. The absorbance was monitored at 710 nm by a diode array spectrophotometer (MOS-200 Optical System, Biologic, Claix, France). Heavy SR vesicles (50 μg) were actively loaded with Ca^{2+} at 37°C in 2 ml of a buffer containing 100 mM KCl, 7.5 mM sodium pyrophosphate, 20 mM MOPS, pH 7.0, supplemented with 250 μM antipyrylazo III, 1 mM ATP/$MgCl_2$, 5 mM phosphocreatine, and 12 μg/ml creatine phosphokinase (25). Ca^{2+} loading was started by sequential additions of 50 and 20 μM of $CaCl_2$. In these loading conditions, no calcium-induced calcium release interferes with the observations. At the end of each experiment, Ca^{2+} remaining in the vesicles was determined by the addition of 4 μM Ca^{2+} ionophore A23187 (Sigma) and the absorbance signal was calibrated by two consecutive additions of 20 μM $CaCl_2$.

Imaging of MCa_b/Strept-Cy3 translocation by confocal microscopy

Imaging on fixed cells

Cell cultures were incubated with 100 nM (final concentration) of the MCa_b/Strept-Cy3 complex in the cell culture medium in the dark and at room temperature unless otherwise stated for 30 min or 1 hr. After three washes with PBS, cells were fixed at room temperature and in the dark by 3% paraformaldehyde during 20 min, washed with PBS and mounted with antifading (Dako) for observation with the confocal microscope. All conditions were compared under identical settings. Samples were analyzed by confocal laser scanning microscopy using a Leica TCS-SP2 operating system. Cy3 fluorescence was excited by using the 543 nm line of a helium-neon laser, and the fluorescence emission was collected from 554 to 625 nm.

Imaging on living cells

Living cells were incubated at room temperature in fresh culture medium on the stage of an upright compound microscope (Eclipse 600 FN, Nikon) equipped with a water immersion 40× objective (numerical aperture 0.8) and a confocal head (PCM 2000, Nikon) or with the Leica TCS-SP2 microscop with a 100× objective under “XYZt” mode. MCa_b/Strept-Cy3 penetration kinetics were followed immediately after injection of 100 nM of this complex into the culture medium. Cy3 fluorescence was excited with the 488 nm wavelength line of an argon laser. Emitted light was filtered by a 595 ± 35 nm filter. Images were acquired and analysed with the EZ2000 software (Nikon). Relative fluorescence quantitative analysis was realized on the stack using the devoted Leica software.

RESULTS

Synthesis of biotinylated MCa and complex formation with Cy3-labeled streptavidine

We have previously identified MCa as a potent activator of the skeletal muscle RyR1 calcium channel (3,4). As RyR1 is an intracellular target, these observations suggested that MCa may modulate RyR1 by one of two mechanisms: (i) indirectly through binding onto a plasma membrane receptor (implies no cell penetration) or (ii) directly through binding onto RyR1 itself (implies cell penetration).

With the recent identification of a RyR1 binding site for MCa (6) and earlier evidence that MCa alters the gating of purified RyR1 channels reconstituted in lipid bilayers, we favour the hypothesis that MCa can reach its intracellular target directly by crossing the plasma membrane. To investigate this question, we synthesized a biotinylated version of MCa (MCa_b) in order to create a fluorescent complex MCa_b coupled to Cy3-labeled streptavidine (MCa_b/Strept-Cy3). We first tested whether biotinylation and complex formation with Strept-Cy3 does not impair the functional effects of MCa on RyR1. Fig. 2 demonstrates that the MCa_b/Strept-Cy3 complex retains the ability to stimulate [^{3}H]-ryanodine binding on SR vesicles (panel A) as well as to induce Ca^{2+} release from SR vesicles (panel B). The slower kinetics of Ca^{2+} release induced by the MCa_b/Strept-Cy3 complex as compared to MCa alone is indicative of a slightly reduced efficiency (Fig. 2B). This difference probably stems from a reduced accessibility of MCa_b/Strept-Cy3 to the active MCa binding site on RyR1 owing to the bulkiness of Strept-Cy3 (molecular weight of streptavidine of 60,000 Da compared to 4,108 Da for MCa_b). However, these data indicate that the formation of a complex with Strept-Cy3 does not alter MCa structure and regulatory function making the MCa_b /Strept-Cy3 complex a valid fluorescent indicator to follow the ability of MCa to penetrate into cells.

Cell penetration of MCa_b/Strept-Cy3 complex

Using the MCa_b/Strept-Cy3 complex, we investigated the ability of MCa to transduce various cell types (Fig. 3). A primary cell culture of hippocampal CA1 neurons, and two cell lines, HEK293 and L6 cells (before and after differentiation), were incubated for 30 min (room temperature) with 100 nM of MCa_b complexed to Strept-Cy3. Cells were then fixed and the fluorescence observed by confocal microscopy. The data demonstrate that all cells are labelled, with a strong and uniform staining at the plasma membrane and the cytoplasm, whereas the nucleus is weakly labelled (Fig. 3). In contrast, cells incubated in the presence of 100 nM non-biotinylated MCa and equivalent concentrations of Strept-Cy3 do not display any labelling demonstrating that Strept-Cy3 alone is not able to transduce into cells. The association of Strept-Cy3 with MCa_b is thus required for the fluorescent complex to enter cells, demonstrating the active function of MCa in this process. These data thus indicate that MCa not only acts as a CPP, but, like many other CPP, has the ability to cargo large molecular weight proteins (streptavidine is 14.6-fold larger than MCa).

Kinetics of cell penetration by the MCa_b/Strept-Cy3 complex

To further characterize the transduction properties of MCa, we analyzed the time course of the fluorescence labelling of living non-differentiated L6 cells by MCa_b/Strept-Cy3 complex. In order to achieve this study, we used time-lapse confocal microscopy in a way that preserves cell integrity and viability over at least a 1 hr period. Cell labelling is evident for periods of time as short as 3 min after the addition of 100 nM MCa_b/Strept-Cy3 complex in the extracellular medium (Fig. 4A). We defined three regions of interest (ROI) corresponding to the plasma membrane (ROI-1), the cytoplasm (ROI-2) and the nucleus (ROI-3). The positioning of the different ROI was facilitated by the analysis of the transmitted light image of the cell under observation (Fig. 4B). We then analyzed the evolution of the fluorescence intensity as a function of time in the different ROI with a Leica confocal microscope under the XYZt mode (Fig. 4C). At the start of application of 100 nM of the MCa_b/Strept-Cy3 complex in the bath, the fluorescence intensity increases in all cell compartments albeit with different rates. The evolution is fastest and greatest for the plasma membrane (ROI-1) and reaches a peak in 10 min. A slower, but nevertheless important, increase in fluorescence is also observed for the cytoplasmic compartment (ROI-2), while a much smaller, but above background, fluorescence increase is observed for the nucleus (ROI-3). The rate and the relative intensity at which fluorescence increases in each compartment is consistent with the direction of progression of the MCa_b/Strept-Cy3 complex within the cell, i.e. from the extracellular space to the plasma membrane, from the plasma membrane to the cytoplasm, and then from the cytoplasm to the nucleus. Of note, the fluorescence signal recorded in ROI-1 corresponds to the fluorescence associated to the plasma membrane plus the cytoplasmic area close to the membrane. Since the signal is normalized, it underestimates the plasma membrane associated fluorescence. In contrast, the relative fluorescence intensity of the cytoplasm should be more accurate. Two conclusions should be drawn from these data. First, the passage of the MCa_b/Strept-Cy3 complex from the cytoplasm to the nucleus is very weak suggesting that this transition is far less favoured than the two other ones. Second, the fluorescence associated to cell compartments is far greater than the fluorescence from the bath demonstrating that cells act as MCa “concentrators”. We also followed the evolution of the fluorescence once the MCa_b/Strept-Cy3 complex was washed out of the bath, i.e. after 12 min of MCa_b/Strept-Cy3 application and 5 min of wash (Fig. 4C). We observed that the fluorescence intensity of ROI-1 decreases whereas that of ROI-2 increases. ROI-3 fluorescence intensity remains constant. The fluorescence increase of the cytoplasmic compartment must thus be related to a continued transfer of the complex from the plasma membrane into the cytoplasm. This plasma membrane/cytoplasm transfer is probably the rate-limiting step in MCa entry. The decrease in fluorescence intensity of the plasma membrane must thus result both from a leakage of the fluorescent complex to the extracellular medium and from its transfer to the cytoplasm. Longer periods of observations were precluded by the appearance of an inhomogeneous distribution of the fluorescent dye in the cytoplasm, maybe linked to degradation pathways (data not shown). However, we conclude from these data that complexes of MCa_b/Strept-Cy3 that have penetrated into cells appear to stably remain inside the cell suggesting that MCa has a favoured direction of plasma membrane crossing.

Endocytosis is not required for translocation of the MCa_b/Strept-Cy3 complex

Several cell mechanisms are known that may allow the entry of MCa. Transduction mechanisms are postulated to be energy-independent and do not require a specific receptor for translocation across the plasma membrane, whereas endocytosis and pinocytosis are energy-dependent. Although a contribution of an endocytotic process is possible, two reasons suggest that it is not the primary mode of entry of MCa. First, the distribution of the MCa_b/Strept-Cy3 complex in the cytoplasm is quite uniform. Second, the normal intracellular target of MCa (RyR1) requires a direct release of MCa into the cytoplasm which is hardly compatible with endocytosis. We nevertheless investigated the contribution of energy-dependent processes in the entry of the MCa_b/Strept-Cy3 complex (Fig. 5). We first tested the effect of decreasing the temperature on the entry of MCa_b/Strept-Cy3 complex (Fig. 5B). The data unambiguously demonstrate that the entry of the complex still occurs at 4°C. At this temperature, the complex similarly labels the plasma membrane and the cytoplasm. Also, we tested the effect of specific inhibitors of pinocytosis and endocytosis. Neither 3 mM amiloride (Fig. 5C) nor 50 μM nystatin (Fig. 5D) had any effect on the cell entry of the complex or its relative distribution in the plasma membrane and in the cytoplasm, again confirming that the main pathway for entry of MCa into cells does not involve either endocytosis or pinocytosis.

DISCUSSION

In this manuscript, we demonstrate that MCa has the ability to translocate into cells by crossing the plasma membrane. This process is rapid since translocation appears evident even for incubation times as short as 1 or 2 min. It reaches saturation in the plasma membrane around 10 min, though longer times were required for entry into the cytoplasm. This is consistent with the kinetics of entry of other CPP with a peak of entry of 15 min for the Tat-p27Kip1 (26) and Tat-β-galactosidase complexes (18).

In our experiments, we coupled MCa_b to streptavidine which is of significantly higher molecular weight than MCa itself, demonstrating that MCa can also carry large molecules into cells, like other CPP (27,28). The fact that MCa_b is so efficient with such a large cargo suggests that uncoupled MCa should be even more efficient when added to the extracellular medium of cells. Indeed, it was observed that Ca^{2+} release from myotubes alone occurred as fast as 3 sec after the addition of MCa, suggesting a much faster translocation in the absence of a cargo molecule. The demonstration that uncoupled MCa has an even faster kinetics of cell entry awaits the synthesis of a fluorescent derivative of MCa. Attempts to produce such a derivative have been unsuccessful so far. In our experiments, we used a concentration of MCa_b (100 nM) that is in the range for which other CPP demonstrate efficient translocation (usually between 25 to 200 nM (17). We show that translocation of MCa occurs at 4°C, as well as in the presence of inhibitors of pinocytosis and endocytosis, demonstrating that the process is energy-independent like for other CPP (17,29,30). Though the current mechanism of MCa translocation is unknown, we can only propose that it may occur along one the mechanisms suggested for other CPP. Like for other CPP, we found that maurocalcine has the ability to effectively translocate in different cell types suggesting that the process is insensitive to the nature of the biological membrane or to the types of receptors expressed on its surface. It is thought that CPP interact with the plasma membrane before translocation through their positively charged surface presumably with negative charges present at the extracellular surface of the lipid bilayer (31). Since MCa also possesses such a positively charged surface, one may assume that it interacts with the lipid bilayer in a manner akin to other CPP. Nevertheless, it should be mentioned that endocytosis may represent an additional contributing factor to MCa cell entry for longer periods of incubation though we did not investigate this question. Referencing the literature, we noticed that all CPP are small peptides. In Tat, the PTD encompasses the basic amino acid residues 47-57 (17,32,33), whereas in VP22 and ANTP, the PTD goes from residues 267-300 (29) and 43-58 (14), respectively. Similarly, the putative PTD sequence of maurocalcine should be shorter than 33 amino acid residues. The sequence of MCa that triggers translocation is unknown. However, owing to its similarities with other CPP, the basic amino acid rich sequence is the principal suspect. One intriguing observation is that part of the same basic sequence involved in translocation also appears to mediate the interaction with RyR1. For instance, mutation of Arg_{24} of MCa, that belongs to the putative CPP sequence, results in a complete loss of interaction with RyR1 (4). Interestingly, part of the PTD of HIV-1 Tat, the Gly-Arg-Lys-Lys-Arg-Arg sequence, is also a potential nuclear localization sequence (12). In addition, Tat, VP22 and ANTP are all proteins implicated in transcriptional regulation, and the PTD are the domains that make contact with nucleic acids. This seems to indicate that PTD may intrinsically possess multiple functions: protein translocation (all CPP), protein targeting (Tat), and protein (MCa) or nucleic acid interaction (Tat, VP22 and ANTP).

Overall, we thus have several arguments to believe that MCa behaves as a CPP. Like recognized CPP sequences: 1- MCa is a small peptide, 2- it is positively charged, 3- it enters many cell types, 4- it enters in an efficient manner, 5- at low concentration, 6- the translocation is a fast process, 7- that is energy-independent, and 8- it can carry a cargo molecule. It possesses yet two other essential properties maybe not shared with other CPP which is i) its apparent capacity to enter cells against its concentration gradient and ii) to enter far more rapidly than to exit the cell. The reasons for these properties are unknown but we tentatively assume that the membrane potential may work as a driving force for cell penetration and maintenance. Because MCa is structured by disulfide bridges, it should be classified as belonging to a new class of CPP. Also, the disulfide linkage of MCa, which makes it more rigid than other CPP, implies that the transduction mechanism at the basis of MCa cell penetration does not rely on extensive peptide unfolding. Owing to the growing importance of CPP in delivering functionally important molecules into cells, the identification of MCa will be useful to further understand the molecular basis of cell penetration of CPP. In addition, MCa may constitute a leading compound for the design of new and efficient

analogues to deliver active drugs inside cells that would otherwise have limited or no bioavailability. A new CPP may be of interest for biotechnological and pharmaceutical companies.

The abbreviations used are

CPP: Cell Penetrating Peptide

EDTA: Ethylenediaminetetraacetic acid

EGTA: Ethyleneglycol-bis(beta-aminoethylether)-N,N′-tetraacetic acid

MCa: Maurocalcine

MCa_b : Biotinylated maurocalcine

PBS: Phosphate Buffered Saline

PTD: Protein Transduction Domain

ROI: Region Of Interest

RyR1: Ryanodine Receptor type 1

SR: Sarcoplasmic Reticulum

Strept-Cy3: Streptavidine-cyanine 3

References:

- 1.. Mosbah A , Kharrat R , Renisio JG , Blanc E , Sabatier JM , El Ayeb M , Darbon H 1998; 6ème Rencontre en Toxinologie. Paris
- 2. Mosbah A , Kharrat R , Fajloun Z , Renisio JG , Blanc E , Sabatier JM , El Ayeb M , Darbon H 2000; Proteins. 40: 436- 442
- 3. Chen L , Estève E , Sabatier JM , Ronjat M , De Waard M , Allen PD , Pessah IN 2003; J Biol Chem. 278: 16095- 16106
- 4. Estève E , Smida-Rezgui S , Sarkozi S , Szegedi C , Regaya I , Chen L , Altafaj X , Rochat H , Allen P , Pessah IN , Marty I , Sabatier JM , Jona I , De Waard M , Ronjat M 2003; J Biol Chem. 278: 37822- 37831
- 5. Fajloun Z , Kharrat R , Chen L , Lecomte C , di Luccio E , Bichet D , El Ayeb M , Rochat H , Allen PD , Pessah IN , De Waard M , Sabatier JM 2000; FEBS Lett. 469: 179- 185
- 6.. Altafaj X , Cheng W , Estève E , Urbani J , Grunwald D , Sabatier JM , Coronado R , De Waard M , Ronjat M 2004; J Biol Chem.
- 7. Green M , Loewenstein PM 1988; Cell. 55: 1179- 1188
- 8. Frankel AD , Pabo CO 1988; Cell. 55: 1189- 1193
- 9. Dorn A , Affolter M , Gehring WJ , Leupin W 1994; Pharmacol Ther. 61: 155- 184
- 10. Lundberg M , Johansson M 2002; Biochem Biophys Res Commun. 291: 367- 371
- 11. Prochiantz A 2000; Curr Opin Cell Biol. 12: 400- 406
- 12. Schwarze SR , Dowdy SF 2000; Trends Pharmacol Sci. 21: 45- 48
- 13. Lundberg P , Langel U 2003; J Mol Recognit. 16: 227- 233
- 14. Derossi D , Joliot AH , Chassaing G , Prochiantz A 1994; J Biol Chem. 269: 10444- 10450
- 15. Pouny Y , Rapaport D , Mor A , Nicolas P , Shai Y 1992; Biochemistry. 31: 12416- 12423
- 16. Gazit E , Lee WJ , Brey PT , Shai Y 1994; Biochemistry. 33: 10681- 10692
- 17. Vives E , Brodin P , Lebleu B 1997; J Biol Chem. 272: 16010- 16017
- 18. Schwarze SR , Ho A , Vocero-Akbani A , Dowdy SF 1999; Science. 285: 1569- 1572
- 19. Gratton JP , Yu J , Griffith JW , Babbitt RW , Scotland RS , Hickey R , Giordano FJ , Sessa WC 2003; Nat Med. 9: 357- 362
- 20. Dunican DJ , Doherty P 2001; Biopolymers. 60: 45- 60
- 21. Merrifield RB 1986; Science. 232: 341- 347
- 22. Kim DH , Onhishi ST , Ikemoto N 1983; J Biol Chem. 258: 9662- 9668
- 23. Marty I , Thevenon D , Scotto C , Groh S , Sainnier S , Robert M , Grunwald D , Villaz M 2000; J Biol Chem. 275: 8206- 8212
- 24. Seigneurin-Venin S , Parrish E , Marty I , Rieger F , Romey G , Villaz M , Garcia L 1996; Experimental Cell Research. 223: 301- 307
- 25. Palade P 1987; J Biol Chem. 262: 6142- 6148
- 26. Nagahara H , Vocero-Akbani AM , Snyder EL , Ho A , Latham DG , Lissy NA , Becker-Hapak M , Ezhevsky SA , Dowdy SF 1998; Nat Med. 4: 1449- 1452
- 27. Anderson DC , Nichols E , Manger R , Woodle D , Barry M , Fritzberg AR 1993; Biochem Biophys Res Commun. 194: 876- 884
- 28. Fawell S , Seery J , Daikh Y , Moore C , Chen LL , Pepinsky B , Barsoum J 1994; Proc Natl Acad Sci USA. 91: 664- 668
- 29. Elliot G , O'Hare P 1997; Cell. 88: 223- 233
- 30. Derossi D , Calvet S , Trembleau A , Brunissen A , Chassaing G , Prochiantz A 1996; J Biol Chem. 271: 18188- 18193
- 31. Lindgren M , Hallbrink M , Prochiantz A , Langel U 2000; Trends Pharmacol Sci. 21: 99- 103
- 32. Mann DA , Frankel AD 1991; EMBO J. 10: 1733- 1739
- 33. Ezhevsky SA , Nagahara H , Vocero-Akbani AM , Gius DR , Wei MC , Dowdy SF 1997; Proc Natl Acad Sci USA. 94: 10699- 10704

Fig. 1

3-D solution structure of several peptides. 3-D solution structure of MCa (Protein Data Bank accession code, 1C6W). Basic amino acid residues present on the same face of MCa are shown (Lys_{11}, Lys_{14}, Lys_{19}, Lys_{20}, Lys_{22}, Arg_{23}, Arg_{24} and Lys_{30}). Lys_{11} belongs to the β-strand 1, Lys_{20}, Lys_{22} and Arg_{23} to the β-strand 2, whereas Lys_{30} belongs to the β-strand 3. The 3-D solution structures of penetratin 1 (accession code 1KZ0), TAT proteins from HIV1 (1TIV) and equine infectious anemia virus (1TVT) are also shown. Lateral chains of basic amino acid residues are highlighted in blue. The primary structures of the peptides are also provided. The pictures are generated with SwissPDB viewer (Swiss-Prot, Switzerland).

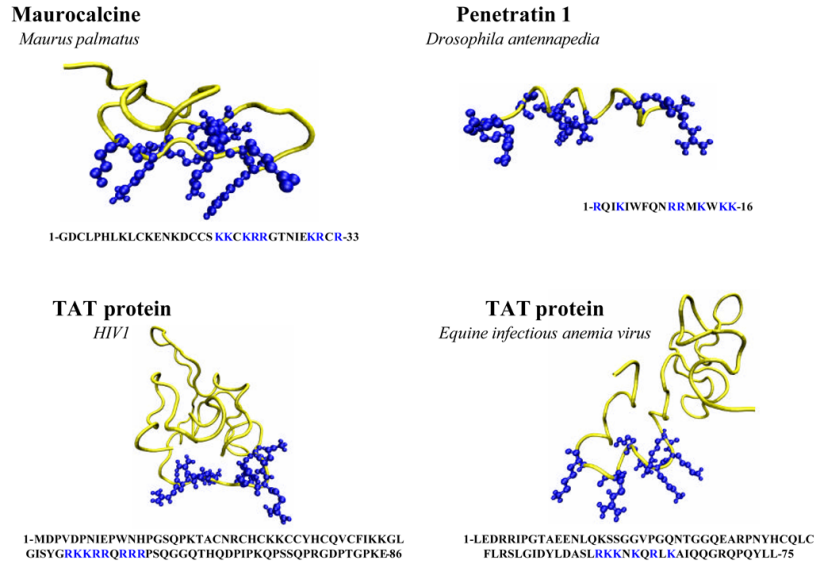


Fig. 2

The MCa_b/Strept-Cy3 complex is functionally active on RyR1. A, Stimulation of [^{3}H]-ryanodine binding by 100 nM MCa or MCa_b /Strept-Cy3 complex. Specific [^{3}H]-ryanodine binding on SR vesicles was measured as described Materials and Methods. Dash represents binding in the absence of MCa or MCa_b/Strept-Cy3 complex. B, Induction of Ca^{2+} release from SR vesicles by 100 nM MCa or MCa_b /Strept-Cy3 complex. 1 and 2 represent addition of 50 and 20 μM $CaCl_2$ (final concentration), whereas 3 and 4 represent the consecutive addition of 20 μM $CaCl_2$. A23187 was added at a final concentration of 4 μM.

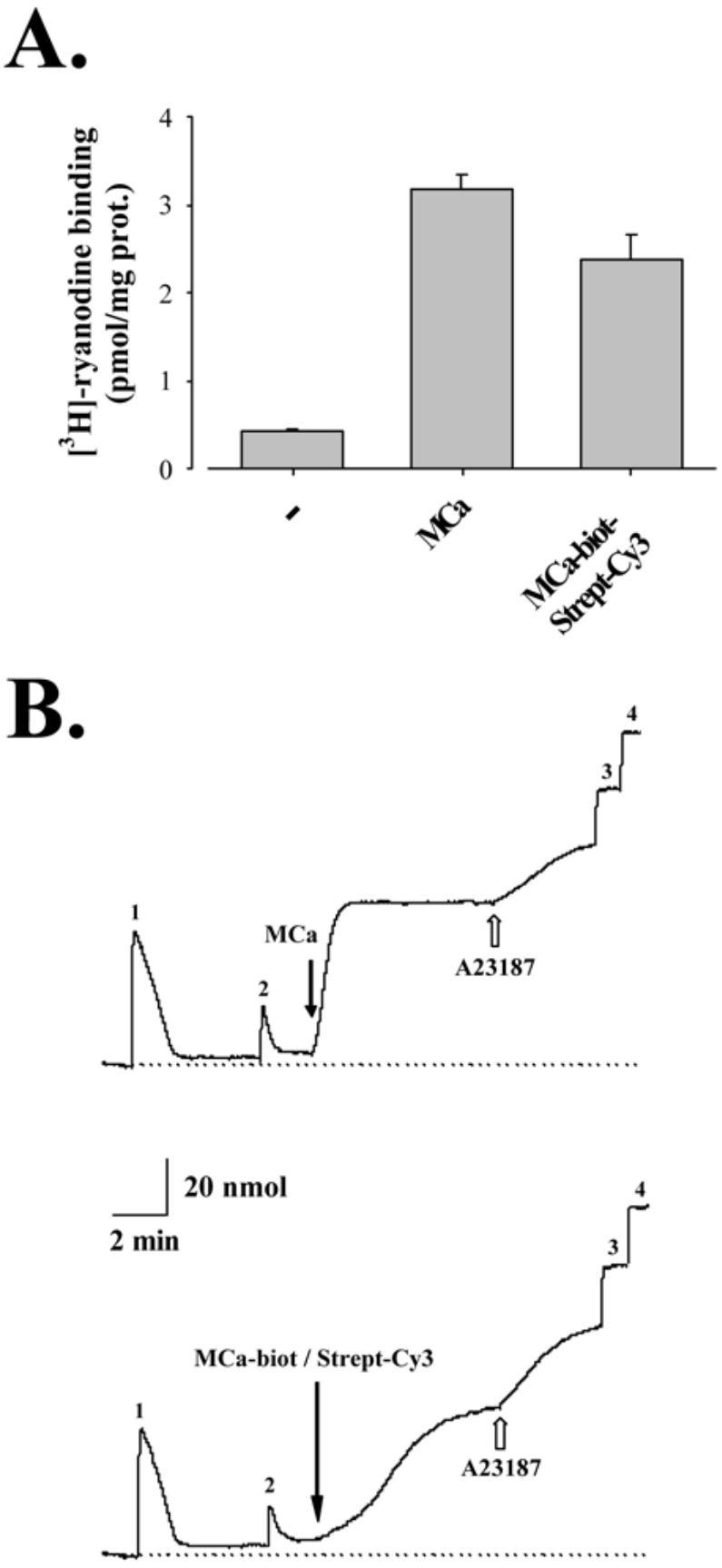


Fig. 3

MCa_b/Strept-Cy3 complex transduces efficiently in many different cell cultures. 3, 2 and 1 day-old cultures of hippocampal CA1 neurons, HEK293 cells and non-differentiated L6 cells, respectively, were incubated for 30 min with 100 nM MCa_b complexed to Strept-Cy3 before fixation and confocal analysis. Differentiated L6 cells were treated similarly (4-days of differentiation). Fourfold smaller panels represent control experiments in which cells were treated with a mixture of 100 nM non-biotinylated MCa and Strept-Cy3.

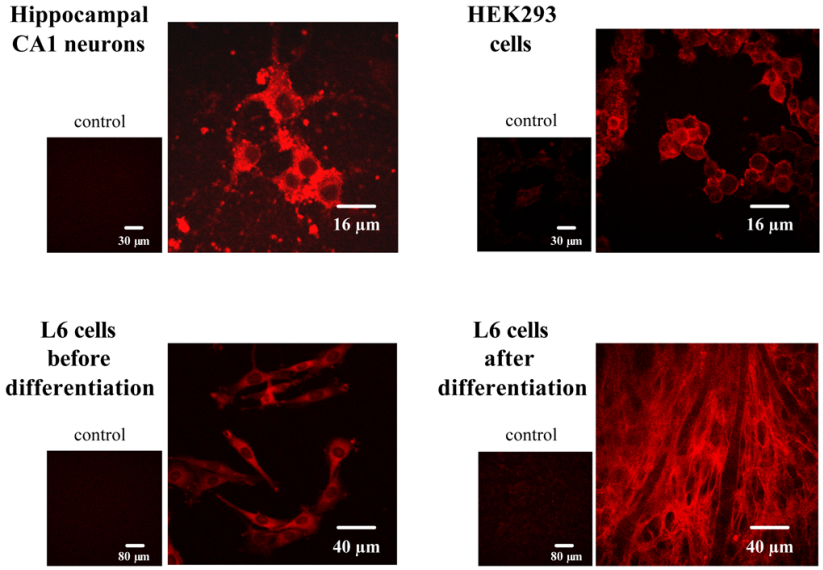


Fig. 4

Kinetic of MCa_b/Strept-Cy3 complex transduction in non differentiated L6 cells. A, Confocal Cy3 fluorescence image of proliferating L6 cell at different times (3 sec, 3 min and 12 min) after addition of 100 nM MCa_b/Strept-Cy3 complex and 23 min after wash of the complex. Settings were such that the bath fluorescence of the complex is not visible. B, Position of the different ROI on the transmitted light image (differential interference contrast, top panel) and resulting position on the corresponding confocal Cy3 fluorescence image. C, Evolution of the Cy3 fluorescence intensity normalized to the unity of ROI surface in the different L6 compartments as a function of time. The MCa_b /Strept-Cy3 complex was applied at a concentration of 100 nM at t=0 min and washed for 5 min out of the bath after t=12 min. Basal ROI represents the fluorescence intensity of the extracellular solution. Data are the mean ± s.d. of n=5 different cells. Similar results were also observed in three different cell preparations.

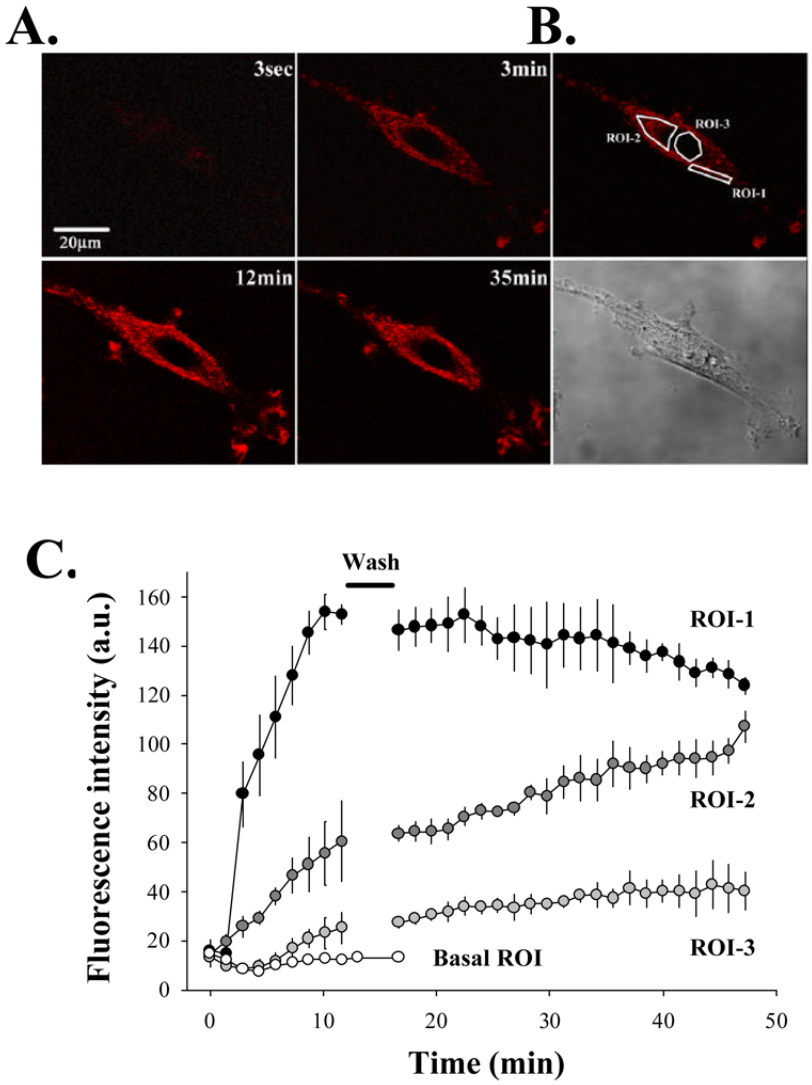


Fig. 5

Cell entry of the MCa_b/Strept-Cy3 complex is energy-independent. A, Control condition for the entry of MCa_b/Strept-Cy3 complex into HEK293 cells. Cells were incubated in the presence of 100 nM of the complex for 1 hr at 22°C. Cells were fixed and images acquired by confocal microscopy. B, Effect of temperature on MCa_b/Strept-Cy3 complex entry. Cells were incubated and observed in similar experimental conditions than at 22°C. C, Effect of 50 μM nystatin on MCa_b/Strept-Cy3 complex entry into HEK293 cells. Nystatin is an inhibitor of pinocytosis. Conditions as in A. D, Effect of 3 mM amiloride on MCa_b/Strept-Cy3 complex entry into HEK293 cells. Amiloride is an inhibitor of caveolae endocytosis. Conditions as in A.

